

Examination of Power Converters with Modulated Switching Frequency

D. Stepins

Institute of Radioelectronics, Riga Technical University,
12 Azenes str., LV-1048 Riga, Latvia, e-mail: stepin2@inbox.lv

Introduction

Nowadays, switching power dc/dc converters (SPC) are crucial in many electronic devices, especially for portable electronics, such as laptops, mobile phones, etc. The advantages of the use of SPC are rather well known - high power efficiency and high volumetric characteristics. Electromagnetic interference (EMI) is considered as a major problem of SPC, firstly, because of conducted EMI that can disturb operation of other devices connected to the same line, secondly, because of radiated EMI that can significantly affect performance of other electronic devices placed nearby [1]. The classical ways to reduce EMI often include the use of input and output filters, shielding, etc [1, 2]. EMI can also be reduced by modulating the switching frequency in random, chaotic or periodic manner [1]. As a result of the switching frequency modulation (SFM), energy of discrete harmonics of unmodulated switching frequency is spread over a wider frequency range, thus peak EMI levels are significantly reduced [2] as it is shown in Fig. 1.

Despite the fact that switching frequency modulation technique has its benefits in reducing EMI, it can cause undesirable side effects, mainly related to output voltage ripples [2–5, 8–10]. In [5] it is even said that the presence of large amplitude component in output voltage ripples nullifies the benefits of sinusoidal SFM. The effect of periodic SFM applied to a buck converter operating in

continuous conduction mode (CCM) was investigated in [3, 4]. It was found out in those papers that SFM induces significant LF ripples in output voltage of a buck converter due to the difference between switching delays of a power MOSFET. In this paper another basic SPC topology – boost converter with periodic SFM is examined in terms of its output voltage ripples.

So, the main goals of the study are firstly, to define the problems related to output voltage ripples of a frequency modulated boost converter, secondly, find out the main causes of the problems and analyze influence of modulation parameters and main non idealities of the boost power stage components, and thirdly, propose some recommendations to ease the problems and verify the results experimentally.

Output voltage ripples for ideal modulated boost converter

In the examination a boost converter (shown in Fig. 2.) is used. To simplify the analysis it is considered that the converter operates in open-loop configuration. Since we are concerned with the output voltage ripples, they will be analyzed both in time and frequency domains.

In order to evaluate effect of SFM on the output voltage ripples, the boost converter with all the ideal components should be considered first. In Fig. 3 simulated output voltage ripples are shown for frequency modulated boost converter operating in both CCM and discontinuous conduction mode (DCM).

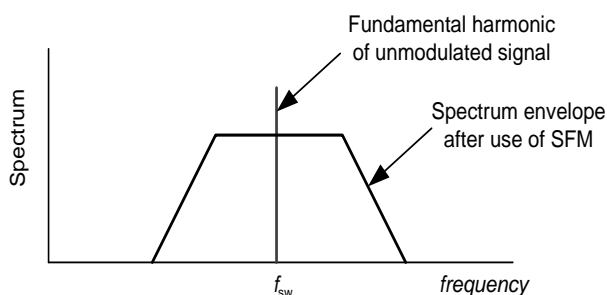


Fig. 1. Simplified spectral structure of a switching signal before and after using SFM

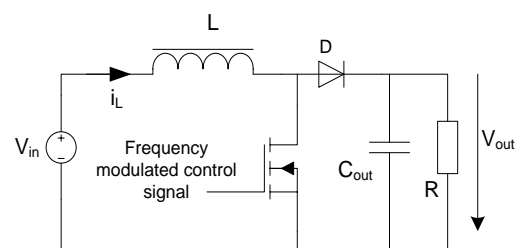


Fig. 2. Boost converter schematics

Increase in peak-to-peak output voltage ripples (ΔV_{outmax}) is evident. For ideal boost converter peak-to-peak ripples are [6]

$$\Delta V_{outmax} = \frac{I_{out}D}{f_{sw}C_{out}}, \quad (1)$$

where I_{out} is DC output current; D is the average duty ratio of the power switch; f_{sw} is the switching frequency of the boost converter.

If f_{sw} is modulated, the ripples change their amplitude according to modulating signal, i.e. they become amplitude and frequency modulated simultaneously. The lower the switching frequency is, the higher the ripples are or vice versa. Maximum output voltage ripples correspond to minimum switching frequency f_{swmin} as follows

$$\Delta V_{outmax} = \frac{I_{out}D}{f_{swmin}C_{out}}, \quad (2)$$

where $f_{swmin} = f_{swc} - \Delta f_{sw}$; f_{swc} is central switching frequency; Δf_{sw} is the switching frequency deviation.

As it can be seen in Fig. 3 the ripples only consist of high-frequency (HF) switching ripples, i.e. low-frequency (LF) component at modulation frequency f_m is not present in output voltage spectrum, as it is also depicted in Fig. 4. The spectrum consists only from sideband harmonics caused by the frequency modulation.

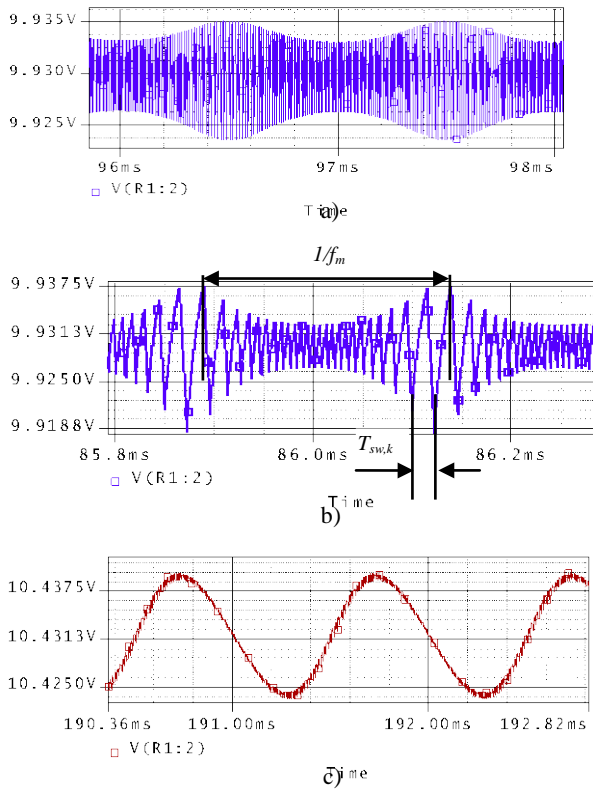


Fig. 3. Output voltage ripple of the ideal SFM boost converter: (a) modulated, CCM ($R_{sw}=200\Omega$, $f_m=1\text{kHz}$; $\Delta f_{sw}=30\text{kHz}$); (b) modulated, CCM ($f_m=4\text{kHz}$; $\Delta f_{sw}=60\text{kHz}$); (c) modulated, DCM ($R_{out}=200\Omega$, $f_m=1\text{kHz}$; $\Delta f_{sw}=30\text{kHz}$). Modulation parameters: sinusoidal modulation; $f_{swc}=100\text{kHz}$. Circuit parameters: $L=125\mu\text{H}$; $C_{out}=330\mu\text{F}$; $V_{in}=7\text{V}$; $D=0.3$

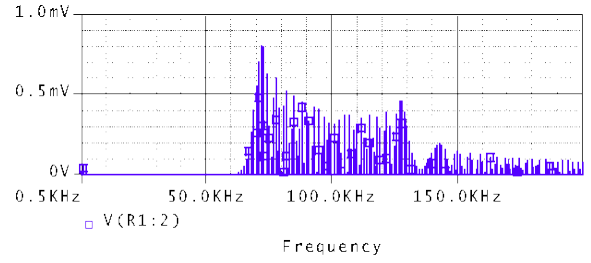


Fig. 4. Simulated spectrum for the output voltage ripples shown in Fig. 3a

However, in DCM the output voltage contain not only the HF switching ripples but also LF variations at f_m , as it is seen in Fig. 3(c). In the spectrum domain this results in the LF components at modulation frequency and its multiples. The difference between these two modes is obvious. In DCM output voltage averaged to the switching period depends on the switching frequency which is modulated. So, in the following we will consider only CCM, but a deep study of the DCM will be dedicated to the further research.

Influence of switching delays

Since the switching delays are very problematic in SFM buck converters in CCM [3,4], effect of SFM on the boost converter output voltage ripples is to be evaluated considering turn-on and turn-off switching delays (t_{don} and t_{doff} respectively) between frequency modulated control signal and the power MOSFET drain-to-source voltage.

Assuming that f_m is always much lower than f_{swc} , average circuit model of the boost converter is used [6] for the theoretical analysis. The state equations for the model are [6]:

$$\begin{cases} L \frac{di_L}{dt} = v_{in} - v_c + v_c d, \\ C_{out} \frac{dv_c}{dt} = (1-d)i_L - v_c / R, \end{cases} \quad (3)$$

where v_{in} , v_c , d and i_L are time-averaged input voltage, the output capacitor voltage, duty cycle and inductor current over one cycle T_{sw} . Replacing the time-averaged values with a DC steady state and small time-varying components and neglecting small-signal and DC products, (3) may be rewritten as [6]:

$$\begin{cases} L \frac{d\tilde{i}_L}{dt} = V_{out}\tilde{d} - (1-D)\tilde{v}_c, \\ C_{out} \frac{d\tilde{v}_c}{dt} = (1-D)\tilde{i}_L - \tilde{v}_c / R - \tilde{d}I_L, \end{cases} \quad (4)$$

where V_{out} is average DC output voltage; I_L is average DC inductor current.

Considering sinusoidal SFM and assuming that $t_{doff} > t_{don}$ (as it usually is), instantaneous duty cycle can be written as [3]

$$d = (D + t_d f_{swc}) + t_d \Delta f_{sw} \sin(\omega_m t), \quad (5)$$

where the difference between the switching delays $t_d=t_{doff}-t_{don}$ and $w_m=2\pi f_m$.

Substituting the time-varying component of duty cycle from (5) to (4) and solving the equation (4), analytical expression for the output capacitor voltage is derived

$$\tilde{v}_c = t_d \Delta f_{sw} \left[(D-1)AV_{out} - w_m^2 L^2 I_L / R \right] \sin(w_m t) + w_m L \cos(w_m t) (AI_L - V_{out}(1-D)/R) / (A^2 + w_m^2 L^2 / R^2), \quad (6)$$

where $A = w_m^2 LC - (1-D)^2$.

Important conclusions can be drawn from (6): if $t_d \neq 0$ the LF ripples are present in the output voltage. Moreover, the LF component is proportional to t_d and Δf_{sw} . After some simplifications of Equation (6) it is also found out that amplitude of the LF variation is approximately inversely proportional to w_m^2 , L and C .

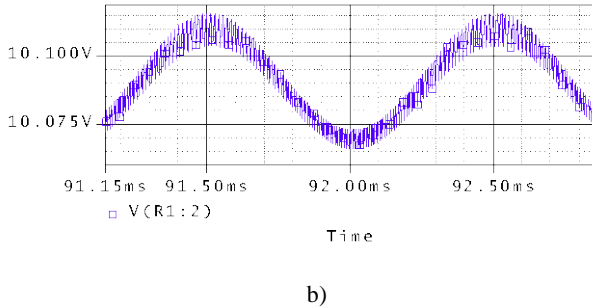
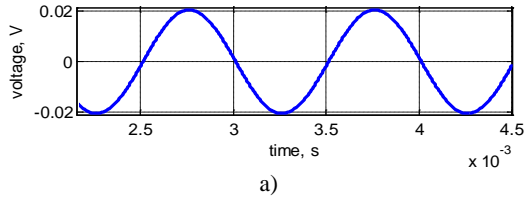


Fig. 5. Calculated LF ripples using (6) (a) and simulated output voltage ripples (b) of the SFM boost converter in CCM ($L=125\mu H$; $C_{out}=330\mu F$; $V_{in}=7V$; $R_{out}=12\Omega$; $D=0.3$; modulation parameters: sinusoidal modulation; $f_{swc}=100kHz$; $f_m=1kHz$; $\Delta f_{sw}=30kHz$; parasitic parameters: $t_d=110ns$)

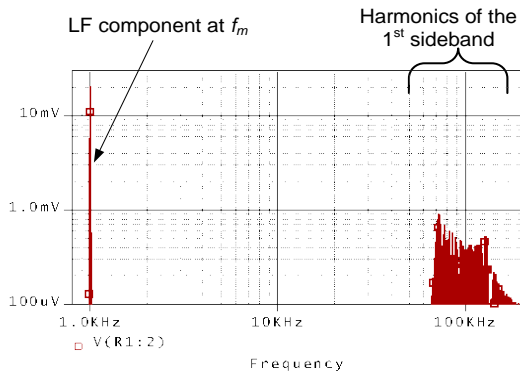


Fig. 6. Simulated spectrum for the output voltage ripples shown in Fig. 5b

In order to verify the theoretical results PSpice boost converter model with adjustable switching delays is used. The simulations for typical values of the modulation and

circuit parameters confirmed Equation (6). As an example, in Fig. 5 the LF variation calculated according to (6) and simulated output voltage ripples are shown for $t_d=110ns$. Because of the LF ripples, component at f_m is now added to the output spectrum (see Fig. 6). It should be noted that the HF switching ripples are not affected by nonzero t_d .

Influence of other main non-idealities

The effect of the switching delays mainly related to the power MOSFET and its driver has been described above. Now it is of interest to investigate the influence of the power MOSFET and diode on resistances (r_{on} and r_d respectively), DC resistance of the power inductor (r_L) as well as the output capacitor equivalent series resistance (ESR, r_c).

HF switching ripples

In order to examine the influence of the power MOSFET, diode and the inductor losses on the output voltage ripples, the same boost converter is simulated with typical values of r_d , r_{on} and r_L . A decrease of several mV in the output voltage ripples was observed for $D=0.3$. However, the decrease is more appreciable for higher D . This is because in the presence of the losses V_{out} and I_{out} decreases [6]

$$I_{out} = \frac{V_{in}}{R} \frac{1-D}{(1-D)^2 + r_{loss}/R}, \quad (7)$$

where $r_{loss} = r_L + Dr_{on} + (1-D)r_d$.

ESR of the output capacitor increases the HF switching ripples appreciably; therefore (2) should be corrected [6]:

$$\Delta V_{out\max} = \frac{I_{out}D}{f_{sw\min}C_{out}} + I_{Lp}r_c, \quad (8)$$

where $I_{Lp} = I_L + \Delta i_L/2$.

As an example in Fig. 7. simulated output voltage ripples of the SFM boost converter are shown for typical values of the losses and ESR. It should be noted that similar problems related to ESR are present in nonmodulated power converters. In fact, the difference between nonmodulated and frequency modulated boost converter maximum output voltage ripples in the presence

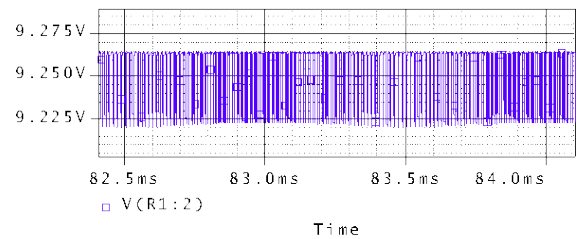
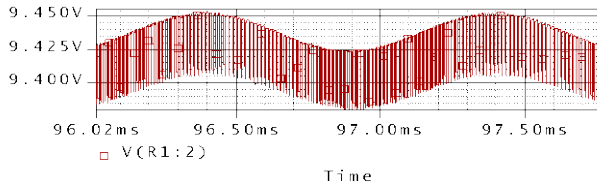
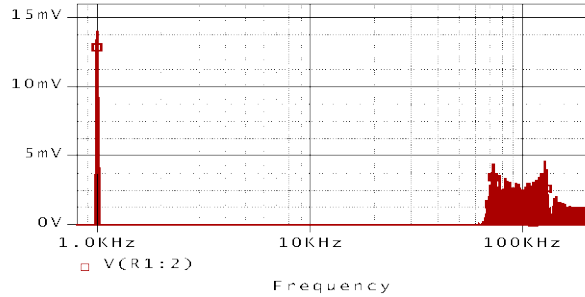


Fig. 7. Simulated output voltage ripples of the SFM boost converter in CCM ($L=125\mu H$; $C_{out}=330\mu F$; $V_{in}=7V$; $R_{out}=12\Omega$; $D=0.3$; modulation parameters: sinusoidal modulation; $f_{swc}=100kHz$; $f_m=1kHz$; $\Delta f_{sw}=30kHz$; parasitic parameters: $t_d=0ns$; $r_{loss}=0.6\Omega$; $r_c=0.035\Omega$)

of ESR is much smaller. This is due to the fact that the



a)



b)

Fig. 8. Simulated output voltage ripples (a) and their spectrum (b) of the SFM boost converter in CCM ($L=125\mu\text{H}$; $C_{out}=330\mu\text{F}$; $V_{in}=7\text{V}$; $R_{out}=12\Omega$; $D=0.3$; modulation parameters: sinusoidal modulation; $f_{swc}=100\text{kHz}$; $f_m=1\text{kHz}$; $\Delta f_{sw}=30\text{kHz}$; parasitic parameters: $t_d=110\text{ns}$; $r_c=0.035\Omega$)

second term in the right of (8) usually has much higher impact on the ripples.

LF ripples

In order to examine influence of r_{loss} and ESR on the LF variation, Equation (4) was rewritten to take them into account. After solving the equations numerically and making simulations of the boost converter with typical values of C_{out} and f_m it is deduced that ESR has less appreciable impact on the LF ripples than on the HF switching ripples. For higher modulation frequencies the effect of ESR is more visible. As an example in Fig. 8 simulated output voltage ripples and their spectrum are depicted for $t_d=110\text{ns}$ and ESR of 0.035Ω .

Experimental verification

Experimental setup. A frequency-modulated dc/dc boost converter (Fig. 9) is designed and built for the verification of the theoretical and simulation results described above. The converter operating in CCM is tested in open loop mode. The input voltage of 7 V is fed from a regulated DC source. A resistor R is connected to the output of the boost converter as a load. The nominal switching frequency is 100kHz.

To perform the switching frequency modulation, a frequency modulated square waveform from an arbitrary waveform generator is fed into driver controlling the power MOSFET. Control signal parameters (i.e. Δf_{sw} , f_{swc} , f_m , D) can be adjusted by the generator. By adjusting the preset resistor $R1$ and the supply voltage of the power MOSFET driver, appropriate switching delays t_{don} and t_{doff}

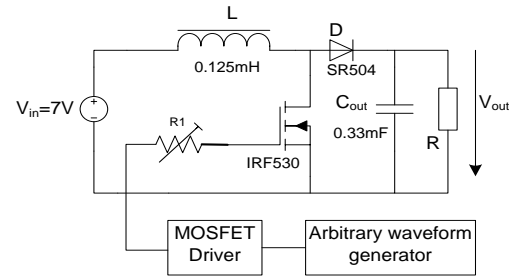


Fig. 9. Simplified schematic diagram of the experimental setup

can be set. For output voltage ripples measurements a digital storage oscilloscope is used.

Experimental results

Measured output voltage waveforms for unmodulated and frequency modulated boost converter are presented in Fig. 10.

Experimental power MOSFET drain-to-source voltage and control signal waveforms are depicted in Fig. 11. Measured spectrum of the output voltage ripples from Fig. 10., b are shown in Fig. 12.

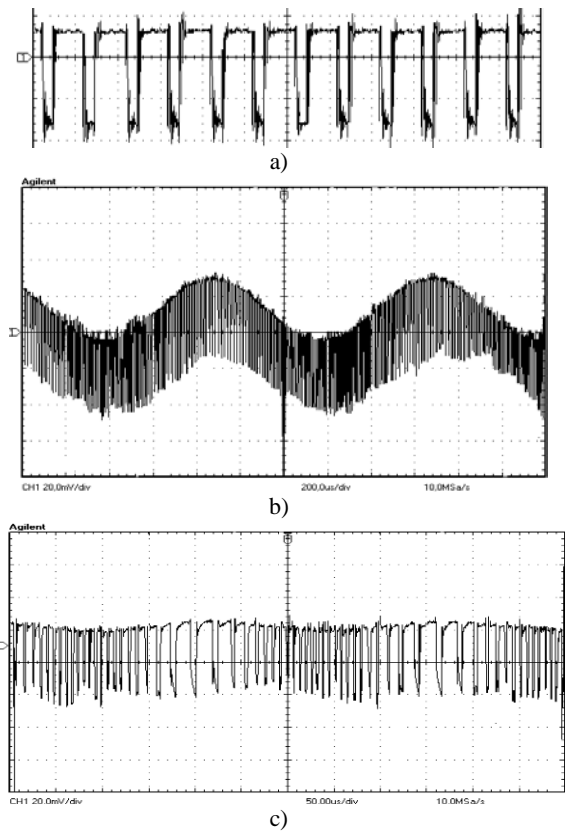


Fig. 10. Measured unmodulated (a) and modulated (b,c) ripples in CCM. Scale: (a) $10\mu\text{s}/\text{div}$, $20\text{mV}/\text{div}$; (b) $200\mu\text{s}/\text{div}$, $20\text{mV}/\text{div}$; (c) $50\mu\text{s}/\text{div}$, $20\text{mV}/\text{div}$. ($L=125\mu\text{H}$; $C_{out}=330\mu\text{F}$; $V_{in}=7\text{V}$; $R_{out}=12\Omega$; $f_{swc}=100\text{kHz}$; $t_d=110\text{ns}$; $r_c=0.035\Omega$ modulation parameters: sinusoidal modulation; (b) $f_m=1\text{kHz}$, $\Delta f_{sw}=30\text{kHz}$; (c) $f_m=4\text{kHz}$, $\Delta f_{sw}=60\text{kHz}$)

Experimental and simulated peak-to-peak output voltage ripples (ΔV_{outmax}) and amplitude (A_{LF}) of the LF variation for the real boost converter with sinusoidal SFM

are summarized in Table 1 for different values of f_m and modulation indexes ($\beta = \Delta f_{sw} / f_m$). In this table the theoretical EMI attenuations (A_{EMI}) for a square waveform with sinusoidally modulated frequency are also shown for a given β value. The attenuations are calculated using the

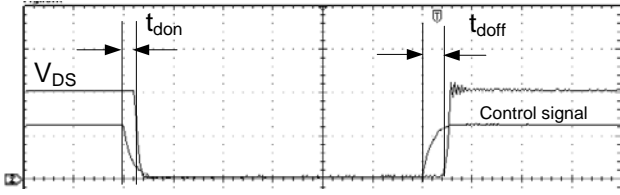


Fig. 11. Measured drain-to-source voltage (V_{DS}) of the power MOSFET and control signal waveforms. Scale: 500ns/div, 5V/div

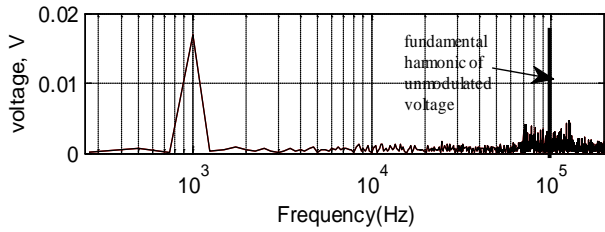


Fig. 12. Experimental spectrum of output voltage ripples in Fig. 10b

Bessel functions [1].

Table 1. Experimental and simulated peak-to-peak output voltage ripples and amplitude (A_{LF}) of the LF variations in CCM ($R_{out}=12\Omega$; $C_{out}=330\mu F$; $L=125\mu H$; $f_{swc}=100kHz$; $\Delta f_{sw}=30kHz$; $t_d=110ns$; $r_c=0.035\Omega$)

f_m , kHz	β	A_{EMI} , dB	Simulated		Experimental	
			ΔV_{outmax} , mV	A_{LF} , mV	ΔV_{outmax} , mV	A_{LF} , mV
1	30	13.3	71	14	75	16
2	15	11.1	49	3.4	53	4.5
5	6	8.8	45	0.63	46	0.85
unmodulated			43	0	44	0

As we can see the experimental results confirm the theoretical predictions and simulation results. Because of nonzero difference between the switching delays, the LF ripples and spectrum component at f_m are present in the output voltage. As f_m increases, the amplitude of the LF ripples appreciably decreases (it is approximately inversely proportional to f_m^2). However increase in f_m leads to decrease in β and consequently worsens EMI attenuation. Despite β can be increased by increasing Δf_{sw} this can be problematic, because the efficiency of the converter could decrease and possible overlap of higher adjacent sidebands can occur [2]. Fortunately the LF ripples can be effectively eliminated, firstly, by proper design of the MOSFET control circuit, keeping the switching delays as equal as possible, and secondly, using proper output voltage feedback control, ensuring f_m falls within the feedback loop bandwidth.

Another method to eliminate the LF ripples is to introduce an artificial delay $t_d = t_{doff} - t_{don}$ to frequency

modulated input signal of the driver for MOSFET turn-on (considering $t_{don} < t_{doff}$). After introducing the delay of 110ns for the driver input signal, the LF variation is practically eliminated even without output voltage control as shown in Fig. 13.

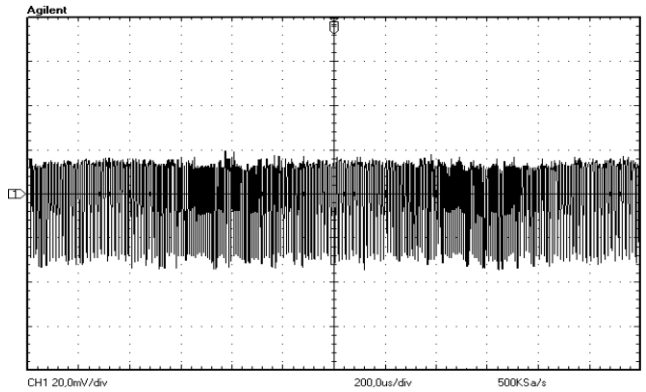


Fig. 13. Measured output voltage ripples in CCM for the SFM boost converter after introducing artificial delay ($t_d=110ns$) for the MOSFET turn-on into the input signal of the driver. Scale: 200 μs /div, 20 mV/div. Modulation and the power stage parameters are the same as in Fig. 10., b. Comparing Fig. 13 and Fig. 10., b, it can be observed that the LF ripples are appreciably decreased after introducing the artificial delay

Conclusions

The effect of periodic switching frequency modulation on a boost converter output voltage ripples has been analyzed in this paper. The output voltage ripples increased after applying SFM, mainly due to the presence of the LF variation at modulation frequency. It is proved that the difference between the power MOSFET switching delays, which are very problematic also in SFM buck converters, is the main cause of the problem. However, the LF ripples can be appreciably decreased by proper design of the power MOSFET control circuit and the use of appropriate output voltage control loop. Increasing modulation frequency can also give good results, but there are some limitations due to EMI attenuation. Additionally, introducing an artificial delay for the power MOSFET turn-on into driver input signal is also very effective method to eliminate the LF ripples. Effect of other non-idealities of the SFM boost converter power stage components (mainly ESR of the output capacitor) on the output voltage is similar to that in unmodulated boost converter. Therefore, choice of the proper output capacitor is also important.

Overall, periodic switching frequency modulation used for EMI suppression has very small influence on worsening quality of the boost converter output voltage, if all the recommendations proposed are considered.

Acknowledgement

This work has been supported by the European Social Fund within the project „Support for the implementation of doctoral studies at Riga Technical University”.

References

1. **Tse K., Chung H., Hui S., So H.** Comparative Study of Carrier-Frequency Modulation Techniques for Conducted EMI Suppression in PWM Converters // IEEE Transactions on Industrial Electronics. – 2002. – Vol. 49. – No. 3. – P. 618–627.
2. **Gonzalez D., Balcells J., Santolaria A., Bunetel J.** Conducted EMI Reduction in Power Converters by Means of Periodic Switching Frequency Modulation // IEEE Transactions on Power Electronics. – 2007. – Vol. 22. – No. 6. – P. 2271–2281
3. **Santolaria A.** Effects of Switching Frequency Modulation on the Power Converter's Output Voltage // IEEE Transactions on Industrial Electronics. – 2009. – Vol. 56. – No. 7. – P. 2729–2737.
4. **Stepins D.** Examination of influence of periodic switching frequency modulation in dc/dc converters on power quality on a load // Proc. of the 11th Biennial Baltic Electronics Conference. – Tallinn, Estonia, 2008. – P. 285–288.
5. **Kultgen M. A.** Spread spectrum modulation of a clock signal for reduction of electromagnetic interference. – U.S. Patent 7417509, 2008.
6. **Erickson R. W.** Fundamentals of Power Electronics, 1st ed. – New York: Chapman and Hall, 1997. – 650 p.
7. **Tse K., Chung H., Hui S., So H.** Spectral Characteristics of Randomly Switched PWM DC/DC Converters Operating in Discontinuous Conduction Mode // IEEE Transactions on Industrial Electronics. – 2000. – Vol. 47. – No. 4. – P. 759–769.
8. **Kuisma M., Jarvelainen T., Silventoinen P.** Analyzing Voltage Ripple in Variable-Frequency DC/DC Boost Converter // in Proc. 35th Annual IEEE PESC. – Aachen, Germany, 2004. – Vol. 1. – P. 1085–1089.
9. **Kairys A., Raudonis V., Simutis R.** “iHouse” for Advanced Environment Control // Electronics and Electrical Engineering. – Kaunas: Technologija, 2010. – No. 4(100). – P. 37–42.
10. **Balsys K., Valinevičius A., Eidukas D.** Traffic Flow Detection and Forecasting // Electronics and Electrical Engineering. – Kaunas: Technologija, 2010. – No. 5(101). – P. 91–94.

Received 2010 02 25

D. Stepins. Examination of Power Converters with Modulated Switching Frequency // Electronics and Electrical Engineering. – Kaunas: Technologija, 2010. – No. 9(105). – P. 33–38.

In this paper analysis of output voltage ripples of a switching frequency modulated (SFM) boost converter operating in continuous conduction mode is performed. The ripples are analyzed in both time and frequency domains theoretically and using computer simulations. Increase in output voltage ripples is observed after using periodic SFM. Low frequency output voltage variation is revealed to be the most problematic. Cause of the problem is found out. Influence of main non-idealities of the boost converter and modulation parameters on the output voltage ripples is also analyzed. Experimental verification is also performed to confirm the theoretical evaluation and simulation results. Some recommendations are given to improve usefulness of periodic SFM in boost converters. Ill. 13, bibl. 10, tabl. 1 (in English; abstracts in English and Lithuanian).

D. Stepins. Galios keitiklių, kuriems veikiant perjungiamas moduliavimo dažnis, tyrimas // Elektronika ir elektrotechnika. – Kaunas: Technologija, 2010. – Nr. 9(105). – P. 33–38.

Nagrinėjamos moduliuojančio dažnio keitiklio išėjimo įtampos pulsacijos nenutrūkstamo veikimo sąlygomis. Laiko ir dažnio atžvilgiu ištirtos pulsacijos, atlikti teoriniai skaičiavimai ir jų rezultatai palyginti su kompiuterinio modeliavimo rezultatais. Nustatyta, kad išėjimo įtampos pulsacijos didėja taikant dažnio moduliaciją netrūkiuoju režimu. Daugiausia problemų kyla dėl įtampos kitimo žemųjų dažnių srityje, kuriam įvertinti atlikta moduliacijos parametrų įtakos išėjimo įtampos pulsacijoms analizė. Atlikti eksperimentiniai tyrimai, patvirtinantys teorinių skaičiavimų ir modeliavimo rezultatus. Pateikiama rekomendacijų. Il. 13, bibl. 10, lent. 1 (anglų kalba; santraukos anglų ir lietuvių k.).